Nanosecond photothermal dynamics in colloidal suspension

R. Kesavamoorthy,[a),b)] Mike S. Super, and Sanford A. Asher[b)]
Department of Chemistry, University of Pittsburgh, Pittsburgh, Pennsylvania 15260

(Received 29 July 1991; accepted for publication 7 October 1991)

Thermal diffusion from a single colloidal sphere suspended in an aqueous medium that is heated by a laser pulse is examined. The temperature field as a function of position and time arising from the cooling of a hot colloidal sphere suspended in an infinitely extended aqueous medium is obtained by solving the heat conduction equation with initial, asymptotic, boundary conditions using a Laplace transform technique. A polymethylmethacrylate sphere of 83 nm diameter is calculated to cool in water within 7 ns. The cooling time is found to decrease quadratically with the particle diameter. We discuss the use of arrays of dyed polymethylmethacrylate spheres suspended in a refractive-index-matched aqueous medium as a fast (ns) optical switching device which acts as an optical monostable.

I. INTRODUCTION

Charged colloidal particles suspended in water form stable dispersions due to their interparticle screened Coulomb repulsive interactions.[1–4] The suspensions exhibit a wide variety of structural ordering and show crystalline, glass, and liquid phases depending on the particle concentration, impurity concentration, particle charge, temperature, and the medium dielectric constant. The crystalline ordering has been exploited to make diffraction devices such as optical rejection filters.[5,6] The colloidal suspension ordering has been investigated using optical microscopy,[7] light scattering,[8] and Bragg diffraction measurements.[9] Scattered and diffracted light intensities depend on the difference in the refractive indices of the particle and the medium.[10,11] These dispersed particle systems have the potential to be used as optical limiters.[12] For example, the colloidal crystals could be prepared from spherical colloids which, at a temperature T_2, have an identical refractive index to the dispersing medium. No diffraction of light will occur from this refractive-index-matched array.[10,11] In contrast, if the sphere were heated by a pulsed laser pump beam that was selectively absorbed by the spheres,[13] a difference in refractive index would occur. The sphere array would selectively diffract until heat diffusion equilibrates the temperature difference.

Here we examine heat diffusion in colloidal suspensions. This contrasts to our previous photothermal studies which examined photothermal compression[13] and photothermal dynamical phenomena[14] in these suspensions. These phenomena resulted from particle motion. We utilize previous thermal diffusion results derived from absorbing solution studies.[15,16] We solve the heat conduction equation for a sphere of polymethylmethacrylate (PMMA) immersed in water heated by a laser pulse, and obtain the temperature field created by a hot colloidal particle cooling in an infinitely extended aqueous medium by solving the heat conduction equation. We calculate the cooling time of the particle and examine its dependence on the particle diameter, and also discuss potential applications of heated index-matched crystalline colloidal arrays of PMMA spheres for use as ns-fast switching devices and optical monostables.

II. THEORY

Consider a polymethylmethacrylate sphere of radius a, mass m_p, and heat capacity C_p at a uniform temperature T_1 at time $t=0$ suspended in water at a temperature T_2 ($< T_1$) everywhere at $t=0$. The quantity of heat contained in the sphere at any time t, $Q(t)$, is given by

$$Q(t)=m_pC_pT_s(t), \tag{1}$$

where $T_s(t)$ is the average temperature of the sphere. The rate of loss of heat from the sphere to the water is given by Newton's law of cooling as

$$-\frac{\partial Q}{\partial t}=\lambda Q, \tag{2}$$

where λ is a constant. The solution of the above equation is given by

$$Q=Ae^{-\lambda t}+B,$$

where the constants A and B are determined from the final and initial conditions,

$$Q|_{t=\infty}=B=m_pC_pT_2,$$

$$Q|_{t=0}=A+B=m_pC_pT_1.$$

Hence,

$$Q=m_pC_p(T_1-T_2)e^{-\lambda t}+m_pC_pT_2, \tag{3a}$$

and comparing the above equation with Eq. (1), the average temperature of the sphere is obtained as

$$T_s=(T_1-T_2)e^{-\lambda t}+T_2. \tag{3b}$$

The heat lost by the sphere in time $t=0$ to t is given by

$$Q_l=Q|_{t=0}-Q|_t.$$

Substituting Eqs. (1) and (3) in the above equation we obtain

[a)]Permanent address: Materials Science Division, Indira Gandhi Center for Atomic Research, Kalpakkam 603102, India.
[b)]Authors to whom correspondence should be addressed.

 0021-8979/92/031116-08$04.00 © 1992 American Institute of Physics

Downloaded 23 Jan 2009 to 130.49.228.46. Redistribution subject to AIP license or copyright; see http://jap.aip.org/jap/copyright.jsp

$$Q_l = m_p C_p (T_1 - T_2)(1 - e^{-\lambda t}). \tag{4}$$

At time $t > 0$, the heat from the particle will diffuse out into the water and the water temperature, $T(t,r)$, will be given by the heat diffusion equation[15]

$$\nabla^2 T = \frac{1}{\alpha}\frac{\partial T}{\partial t}, \tag{5}$$

where α is the thermal diffusivity of water. The present heat diffusion geometry is spherically symmetric and hence Eq. (1) reduces to

$$\frac{1}{r^2}\frac{\partial}{\partial r}\left(r^2 \frac{\partial T}{\partial r}\right) = \frac{1}{\alpha}\frac{\partial T}{\partial t}, \tag{6}$$

where r is the distance from the center of the particle. We solve this expression by substituting the variable u, defined by

$$u(r,t) = rT. \tag{7}$$

Thus,

$$\frac{\partial^2 u}{\partial r^2} = \frac{1}{\alpha}\frac{\partial u}{\partial t}. \tag{8}$$

The solution to the above equation can be readily obtained through the Laplace transform. The Laplace transform of $u(r,t)$ is defined as[17]

$$\bar{u}(r,s) = \int_0^\infty u(r,t) e^{-st} dt.$$

The Laplace transforms of the derivatives of u are given by

$$\overline{\frac{\partial u}{\partial t}} = \int_0^\infty \frac{\partial u}{\partial t} e^{-st} dt = s\bar{u} - u(r,0) \quad \text{and} \quad \overline{\frac{\partial^2 u}{\partial r^2}} = \frac{\partial^2 \bar{u}}{\partial r^2}.$$

The Laplace transform of Eq. (8) becomes

$$\frac{\partial^2 \bar{u}}{\partial r^2} = \frac{s}{\alpha}\left(\bar{u} - \frac{u(r,0)}{s}\right). \tag{9}$$

The temperature of water at $t = 0$ is T_2 everywhere and hence

$$u(r,0) = rT_2, \tag{10}$$

for $r > a$ where a is the sphere radius.

Substituting Eq. (10) in (9) we obtain for $r > a$,

$$\frac{\partial^2 \bar{u}}{\partial r^2} = \frac{s}{\alpha}\left(\bar{u} - \frac{rT_2}{s}\right),$$

the solution of which is given by

$$\bar{u} = C_1 e^{qr} + C_2 e^{-qr} + (rT_2/s), \tag{11}$$

where C_1 and C_2 are the constants in r and $q = \sqrt{(s/\alpha)}$. The constants can be determined from the boundary condition and the continuity equation.

Since $\bar{u}$ must be finite as $r \to \infty$, $C_1 = 0$ and Eq. (11) becomes

$$\bar{u} = C_2 e^{-qr} + (rT_2/s). \tag{12}$$

The heat gained by water from $t = 0$ to t is given by

$$Q_g = \int_a^\infty 4\pi r^2 \rho C[T(r,t) - T_2] dr, \tag{13}$$

where C and ρ are the heat capacity and density of water, respectively. Substituting Eq. (12) in the Laplace transform of Eq. (13) and carrying out the integration, we obtain

$$\bar{Q}_g = (4\pi k C_2 e^{-qa}/s)(1 + qa), \tag{14}$$

where k is the conductivity of water given by

$$k = \rho C \alpha.$$

The heat lost by the sphere from $t = 0$ to t is given by Eq. (4). The continuity equation demands that $Q_g = Q_l$ which implies that

$$\bar{Q}_g = \bar{Q}_l.$$

By comparing Eq. (14) with the Laplace transform of Eq. (4) we obtain

$$\frac{4\pi k C_2 e^{-qa}(1 + qa)}{s} = m_p C_p (T_1 - T_2)\left(\frac{1}{s} - \frac{1}{\lambda + s}\right).$$

The above equation gives the expression for C_2 as

$$C_2 = \frac{\lambda m_p C_p (T_1 - T_2) e^{qa}}{4\pi k(\lambda + s)(1 + qa)}.$$

Hence,

$$\frac{\bar{u}}{r} = \bar{T} = \frac{\lambda m_p C_p (T_1 - T_2) e^{-q(r-a)}}{4\pi k r(\lambda + s)(1 + qa)} + \frac{T_2}{s}. \tag{15}$$

λ is the effective time constant with which the heat content of the particle is decreasing. The value of λ is determined by the rates of heat diffusion within the sphere and/or into the water environment. If the diffusivity of the sphere is much larger than of water, λ will be specified by the heat diffusivity of water and vice versa.

Consider a temperature distribution in the sphere. The thermal equilibration time of the sphere is obtained using Refs. 15 and 18 as

$$t_T \sim a^2/6\alpha_p, \tag{16}$$

where α_p is the thermal diffusivity of the sphere. If $\alpha \gg \alpha_p$, the rate of heat lost by the particle will be limited by the thermal diffusion within the sphere and hence

$$\lambda \sim t_T^{-1}. \tag{17}$$

If $\alpha \ll \alpha_p$, then the sphere can equilibrate faster than the rate of heat transport in water. In such case, λ will be decided by imposing a boundary condition at $r = a$ that

$$T|_{r=a} \leqslant T_p|_{r=a}, \tag{18}$$

where $T_p|_{r=a}$ is the surface temperature of the sphere. This inequality implies that the source temperature cannot be lower than the sink temperature.

In our present case, the values of α and α_p are comparable. Hence we have to examine the values of λ using both methods and choose the lower one. In order to resolve inequality (18), we need to solve the heat conduction equation in the sphere.

Downloaded 23 Jan 2009 to 130.49.228.46. Redistribution subject to AIP license or copyright; see http://jap.aip.org/jap/copyright.jsp

Following the procedure used in this work, we obtain

$$\frac{\partial^2 \bar{u}_p}{\partial r^2}=\frac{s}{\alpha_p}\left(\bar{u}_p-\frac{u_p(r,0)}{s}\right), \tag{19}$$

where the subscript p in u_p and α_p denotes particle. The temperature of the sphere at $t=0$ is T_1 everywhere.

Hence,

$$u_p(r,0)=rT_1. \tag{20}$$

Substituting Eq. (20) in Eq. (19) we obtain

$$\frac{\partial^2 \bar{u}_p}{\partial r^2}=\frac{s}{\alpha_p}\left(\bar{u}_p-\frac{rT_1}{s}\right). \tag{21}$$

The solution of Eq. (21) is given by

$$\bar{u}_p=C_{p1}e^{q_p r}+C_{p2}e^{-q_p r}+\frac{rT_1}{s}, \tag{22}$$

where C_{p1} and C_{p2} are the constants in r and $q_p = \sqrt{(s/\alpha_p)}$. The constants are determined from the boundary condition and heat continuity equation. T_p at $r=0$ is finite at all times. This implies that

$$\bar{T}_p|_{r=0}=\text{finite}.$$

From Eq. (22),

$$\bar{T}_p|_{r=0}=C_{p1}\frac{e^{q_p r}}{r}+C_{ps}\frac{e^{-q_p r}}{r}+\frac{T_1}{s}\bigg|_{r=0}=\text{finite},$$

which gives $C_{p1} = -C_{p2}$.

Hence, Eq. (22) becomes

$$\bar{u}_p=C_{p1}(e^{q_p r}-e^{-q_p r})+(rT_1/s). \tag{23}$$

Heat lost by the sphere from time 0 to t can be written as

$$Q_l=\int_0^a 4\pi r^2 \rho_p C_p[T_1-T_p(r,t)]dr. \tag{24}$$

Substituting Eq. (23) in the Laplace transform of Eq. (24), we obtain

$$\bar{Q}_l=\frac{4\pi\rho_p C_p C_{p1}}{q^2}[e^{q_p a}(1-q_p a)-e^{-q_p a}(1+q_p a)],$$

and comparing the above equation with the Laplace transform of Eq. (4), we obtain

$$C_{p1}=\frac{\lambda m_p C_p(T_1-T_2)}{4\pi k_p(\lambda+s)[e^{q_p a}(1-q_p a)-e^{-q_p a}(1+q_p a)]}. \tag{25}$$

Thus, the temperature of the sphere at any distance and at any time is given by the inverse Laplace transform of

$$\frac{\bar{u}_p}{r}=\bar{T}_p$$

$$=\frac{T_1}{s}+\frac{\lambda m_p C_p(T_1-T_2)(e^{-q_p(a-r)}-e^{-q_p(a+r)})}{4\pi k_p r(\lambda+s)[(1-q_p a)-e^{-2q_p a}(1+q_p a)]}. \tag{26}$$

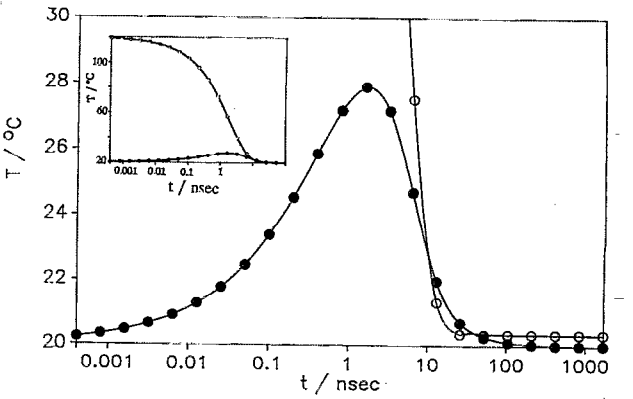

FIG. 1. Calculated sphere surface temperature (○) and water temperature at sphere surface (●) for $\lambda = 3 \times 10^8\ s^{-1}$ as a function of cooling time. Diameter of the sphere is 83 nm. Inset shows the calculated sphere surface temperature and water temperature in an expanded scale.

Hence, the Laplace transform of the surface temperature of the sphere is given by

$$\frac{\bar{u}_p}{r}\bigg|_{r=a}=\bar{T}_p|_a$$

$$=\frac{T_1}{s}$$

$$+\frac{\lambda m_p C_p(T_1-T_2)(1-e^{-2q_p a})}{4\pi k_p a(\lambda+s)[(1-q_p a)-e^{-2q_p a}(1+q_p a)]}. \tag{27}$$

Using Eq. (15), the Laplace transform of the water temperature at the contact with the sphere can be obtained as

$$\bar{T}|_a=\frac{T_2}{s}+\frac{\lambda m_p C_p(T_1-T_2)}{4\pi k a(\lambda+s)(1+qa)}. \tag{28}$$

The inverse Laplace transforms of Eqs. (27) and (28) give $T_p|_{r=a}$ and $T|_a$. We can determine the upper limit of λ for which inequality (18) is satisfied. Comparing this value of λ with that of Eq. (17), we choose the lower value.

III. RESULTS AND DISCUSSION

We assume that the sphere temperature increases uniformly and instantaneously by 100 °C. As indicated below, this temperature increase derives from heating by an incident laser pulse that is selectively absorbed by the spheres. We obtain the value of λ by searching for the minimum value of λ that fulfills the inequality of Eq. (18). Our first guess of λ utilizes the particle thermal equilibration time t_T calculated from Eq. (16); λ is the inverse of $t_T = 3.33 \times 10^{-9}$ s for a PMMA particle of 83 nm diameter ($\lambda = 3 \times 10^8\ s^{-1}$). Using this value of λ, the surface temperature of the sphere and the water temperature at contact with the sphere were calculated by numerically calculating the inverse Laplace transform of Eqs. (27) and (28).

Figure 1 plots these temperatures as a function of time. At time $t=0$, the water temperature is 20 °C. In contrast,

Downloaded 23 Jan 2009 to 130.49.228.46. Redistribution subject to AIP license or copyright; see http://jap.aip.org/jap/copyright.jsp

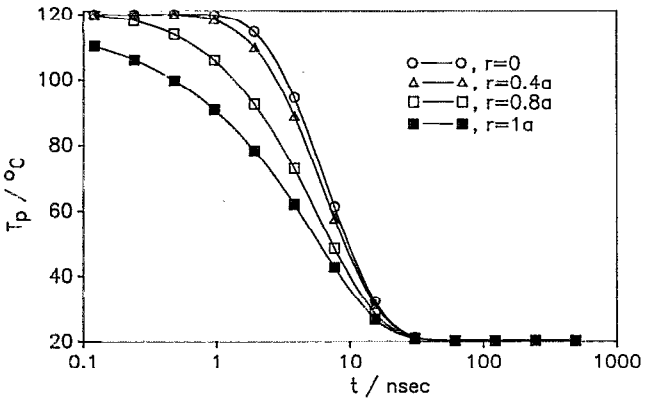

FIG. 2. Calculated sphere temperature at a distance $r=0$ (center of the sphere) (○), $r=0.4a$ (△), $r=0.8a$ (□) and $r=a$ (■) for $\lambda = 1.6 \times 10^8\ s^{-1}$ as a function of time. Diameter of the sphere is $2a = 83$ nm.

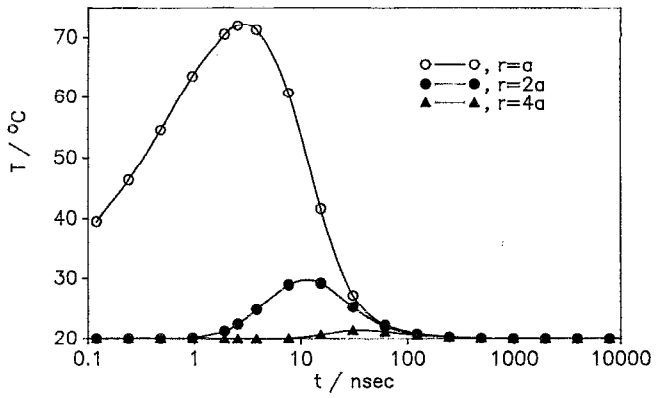

FIG. 3. Temporal dependence of the water temperature at a distance of $r=a$ (○), $r=2a$ (●), and $r=4a$ (▲), from the sphere center. $\lambda = 1.6 \times 10^8\ s^{-1}$, sphere diameter is $2a = 83$ nm.

at $t=0$, the 83-nm-diam polymethylmethacrylate (PMMA) sphere temperature is 120 °C. Figure 1 shows that the particle surface temperature drops to ambient within about 10 ns while the water temperature at the sphere surface increases by 28 °C within 1 ns and decreases to ambient temperature in about 30 ns. The water temperature at the sphere surface is higher than the sphere surface temperature between 10 and 50 ns (Fig. 1), which violates the inequality condition (18). Hence λ is reduced from $3 \times 10^8\ s^{-1}$, until the inequality (18) is satisfied. It was found that $\lambda = 1.6 \times 10^8\ s^{-1}$ just satisfies inequality (18), and hence this value of λ was chosen for the 83-nm-diam PMMA particle cooling in water.

The water temperature and the sphere temperature at various distances and times were calculated by inverse Laplace transforming equations (15) and (26). Figure 2 shows the sphere temperature as a function of time at various radial distances. The particle surface temperature decreases to its $1/e$ value in about 7 ns, while at $r=0$, the temperature decreases to its $1/e$ values by 10 ns. The surface temperature decreases by 10 °C within 0.1 ns while the center temperature takes about 3 ns to decrease by 10 °C.

Figure 3 shows the water temperature as a function of time at different radial distances. The water temperature at contact reaches its maximum temperature rise of 5 °C within 3 ns and decreases to a $1/e$ value in about 17 ns. The temperature excursion at larger distances from the sphere occurs later in time and is smaller in magnitude.

Figure 4 shows the temporal temperature dependence of the sphere and water as a function of the radial distance from the sphere center. At $r=a$, the temperature is discontinuous and the particle cools to 20% of its $t=0$ maximum temperature rise within about 10 ns. The water temperature increase is relatively small ($\sim$5 °C) compared to the particle temperature increase.

Similar cooling curves for different diameter PMMA spheres require different values of λ. For example, λ for 166-nm-diam spheres was found to be $4 \times 10^7\ s^{-1}$ while λ is $6.7 \times 10^8\ s^{-1}$ for 41.5-nm-diam particles. Figures 5(a) and 5(b) show the sphere temperature as a function of time at different radial distances for 166- and 41.5-nm-diam spheres, respectively. It is clear that smaller particles cool faster than larger particles. Figures 6(a) and 6(b) show the water temperature as a function of time at different distances for these two particles. The smaller spheres thermally equilibrate faster than the larger spheres. The maximum water temperature ($\sim$25 °C) occurs at the sphere surface. The calculated value of λ decreases almost as the square of the particle diameter, in agreement with the thermal equilibration time expectations of Eq. (16).

IV. APPLICATIONS

The fast transient temperature response of these spherical particles can be used to create a fast (ns) optical switch. We discuss here an example that utilizes charged 83-nm PMMA spheres containing absorbing but nonemitting dye molecules. The colloidal particles are ordered in a colloidal crystalline array in a refractive-index-matched medium containing a mixture of water and methyl phenylsulfoxide (MPSO), for example. The refractive index[19] of PMMA ($\sim$1.492) at 293 K is identical to that of a solu-

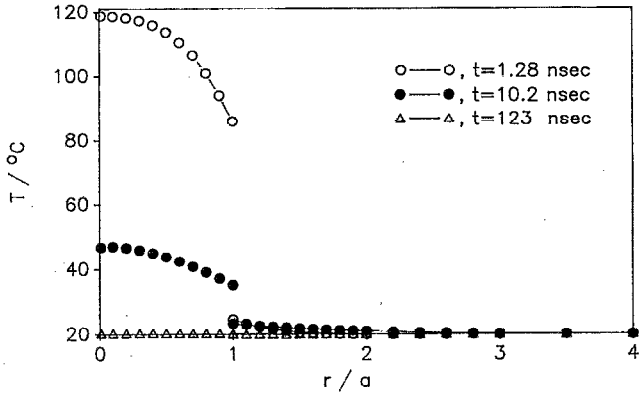

FIG. 4. Particle temperature and water temperature as a function of distance from the sphere center at $t=1.28$ ns (○), $t=10.2$ ns (●), and $t=123$ ns (△). $\lambda = 1.6 \times 10^8\ s^{-1}$, sphere diameter is $2a = 83$ nm.

Downloaded 23 Jan 2009 to 130.49.228.46. Redistribution subject to AIP license or copyright; see http://jap.aip.org/jap/copyright.jsp

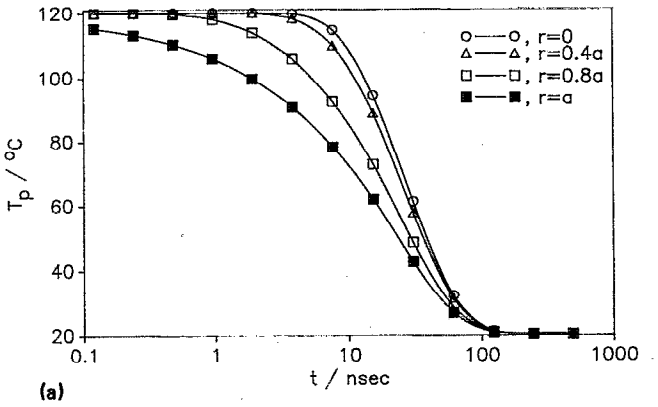

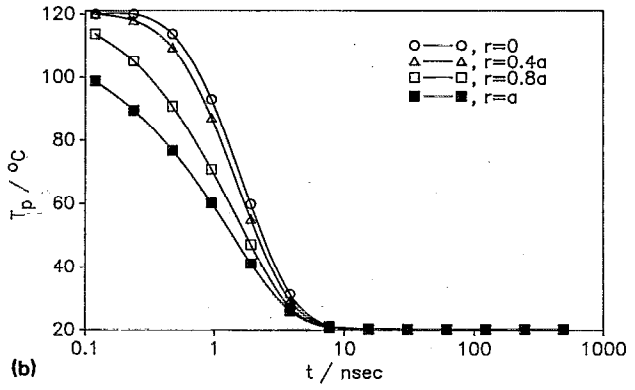

FIG. 5. Sphere temperature at a distance $r=0$ (○), $r=0.4a$ (△), $r=0.8a$ (□), and $r=a$ (■) as a function of cooling time for particle diameter of (a) 166 nm with $\lambda = 4 \times 10^7\ s^{-1}$ and (b) 41.5 nm with $\lambda = 6.7 \times 10^8\ s^{-1}$.

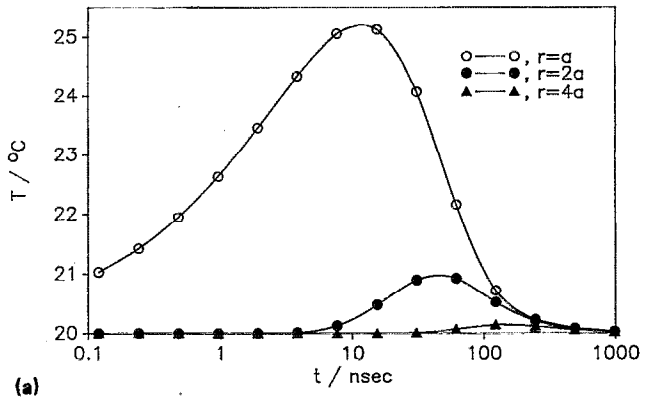

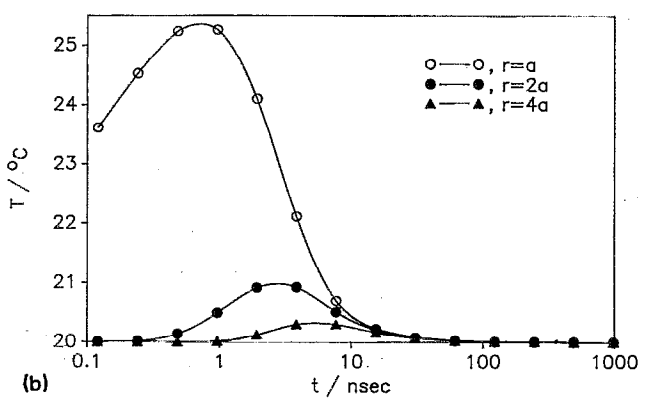

FIG. 6. Temporal dependence of water temperature at a distance of $r=a$ (○), $r=2a$ (●), and $r=4a$ (▲) from the sphere center for particle diameter of (a) 166 nm with $\lambda = 4 \times 10^7\ s^{-1}$ and (b) 41.5 nm with $\lambda = 6.7 \times 10^8\ s^{-1}$.

tion containing 62.2% MPSO (refractive index[20] ~1.570) and 37.8% water (refractive index ~1.323). This colloidal array will, thus, not Bragg diffract light due to the refractive index match between the spheres and the medium. When the suspension is irradiated with a laser pulse absorbed by the dye, the particle temperature will increase relative to that of medium. Since the temperature derivative of the refractive index[19] of PMMA is -1.1×10^{-4}/K, the refractive index mismatch $|\Delta n|$ will increase with temperature. As the refractive index of the sphere diverges from that of the medium, the colloidal crystal will Bragg diffract and the transmission will decrease for light meeting the Bragg condition. The transition from high transmission to low transmission occurs within a few ns. Thus, this device acts as a ns-fast optical switching device.

The low transmission state continues for a period of about 10 ns after the heating beam is turned off during which the thermal inhomogeneity decays and the colloidal crystal recovers to become completely transparent. This device acts as an optical monostable whose dwell time in the unstable state (low transmission state) can be controlled by varying the particle size or the heat beam intensity.

We can calculate transmission of the beam through the colloidal crystal for various incident laser heat beam intensities and durations when the Bragg condition is satisfied. Consider the index-matched PMMA colloidal crystal heated by an incident beam of wavelength λ_h. The resulting index mismatch causes Bragg diffraction of a probe beam of wavelength λ_p if it satisfies the Bragg condition. The ratio between the Bragg diffracted power P_H and the incident power P_0 of the beam from a defect-free colloidal crystal is given by[11]

$$\frac{P_H}{P_0} = \frac{\sinh^2(A\sqrt{1-y^2})}{1-y^2+\sinh^2(A\sqrt{1-y^2})}, \tag{29}$$

with

$$y=(2\psi_0-\alpha)/2|\psi_H| \tag{30}$$

and

$$\alpha=2(\theta_B-\theta)\sin 2\theta_B,$$

where θ_B is the Bragg angle, θ is the incidence angle, ψ_0 is the average crystal polarizability, and ψ_H is the Fourier component of the crystal polarizability with the periodicity of Bragg wave vector, $Q = 4\pi n_s \sin\theta_B/\lambda_p$, where n_s is the suspension refractive index. ψ_0 is obtained from the optical attenuation spectra of the colloidal crystal at various incidence angles.[9,13] ψ_H is given by[21]

$$\psi_H=\phi[(n_{pa}^2/n_m^2)-1]G, \tag{31}$$

Downloaded 23 Jan 2009 to 130.49.228.46. Redistribution subject to AIP license or copyright; see http://jap.aip.org/jap/copyright.jsp

where ϕ is the volume fraction of the particle in the suspension, n_m and n_{pa} are the refractive indices of the medium and the particle, respectively, and G is the particle structure factor given by[21]

$$G=[3\ (\sin Qa - Qa\cos Qa)/Q^3a^3]. \tag{32}$$

The parameter A in Eq. (29) is given by

$$A=2\pi^2 n_s|\psi_H| l_0/\lambda_p \sin\theta_B, \tag{33}$$

where l_0 is the thickness of the crystal.

Let I_0 and t_h be the intensity and pulse duration of the heat beam. Assuming that 1% of the light falling on the particle is completely absorbed (the particle absorption cross section is $\pi a^2/100$), the temperature increase of the particle $\Delta T_p(z)$ at a distance z from the front face of the crystal is given by[15]

$$\Delta T_p(z)=\frac{I_0 t_h \pi a^2}{100 m_p C_p} e^{-n_p\int_0^z C_e(z')dz'} \tag{34}$$

where $C_e(z)$ is the extinction cross section for the heat beam at z which is given by

$$C_e(z)=C_s(z)+(\pi a^2/100), \tag{35}$$

where $C_s(z)$ is the scattering cross section. For a vertically polarized heat beam $C_s(z)$ is given by[10]

$$C_s(z)=\int_{\theta=0}^{\pi}\frac{32\pi^5 n_s^4 a^6}{\lambda_h^4}\left(\frac{n_{pa}^2-n_m^2}{n_{pa}^2+2n_m^2}\right)^2 G(\theta)\sin\theta\, d\theta, \tag{36}$$

where $G(\theta)$ is given by Eq. (32) with the scattering angle $\theta = 2\theta_B$. The computed value of $C_s(z)$ using the above equation is found to be about four orders of magnitude smaller than πa^2. The refractive index mismatch between the particle at z and the medium, $\Delta n(z)$, induced by $\Delta T_p(z)$ is given by[19]

$$\Delta n(z)=-1.1\times 10^{-4}\Delta T_p(z), \tag{37}$$

where $dn/dT = -1.1\times 10^{-4}\ \mathrm{K}^{-1}$ for PMMA particles. Since the heat beam is attenuated in the suspension, $\Delta n(z)$ will be a function of z and hence the effective value of a A is obtained from Eqs. (33) and (31) by integration and is given by

$$A=\int_0^{l_0}\frac{2\pi^2 n_s G\phi}{\lambda_p\sin\theta_B}\left(\frac{n_{pa}^2(z)}{n_m^2}-1\right)dz. \tag{38}$$

The minimum transmission that occurs for $y=0$ in Eq. (29) of an incident beam satisfying the Bragg condition (probe beam) can be calculated from Eqs. (29)–(38). Table I gives the transmission of the probe beam of $\lambda_p = 514.5$ nm ($P_t/P_0 = 1 - P_H/P_0$) through a 400-μm-thick dyed index-matched PMMA colloidal crystal for various incident laser pulse intensities and Bragg angles. The transmittance P_t/P_0 decreases as I_0, t_h, and θ_B increases. Figure 7 shows that the transmission of the probe beam is a nonlinear function of heat beam intensity. Figure 8 shows the transmission of the probe beam as a function of time for a 5-ns-wide rectangular heating beam of 10 MW/cm^2. If the switching of the state (device) is defined as the time to reach the 0.5 transmission point, then Fig. 8 demonstrates a switching time of 2 ns and a monostable time constant of ~9 ns. Thus, the dyed index-matched PMMA colloidal crystal can be used as an optical switching device that turns on in 2 ns and operates as an optical monostable. This device could serve as an optical switch that can trigger the simultaneous transmittance decrease of multiple beams through the device. In this case, different wavelength would pass through the device at their individual Bragg angles. The transmission of all of these beams could be simultaneously switched off by a single heat beam.

TABLE I. Transmittance of a beam satisfying the Bragg condition at angle θ_B in an index-matched bcc colloidal crystal consisting of 83-nm-diam PMMA particles heated by incident laser pulses of intensities I_0 with pulse durations t_h.

I_0 (MW/cm^2)	t_h (ns)	θ_B	P_t/P_0
1	10	75	0.8451
5	10	75	0.0605
10	10	75	0.0010
1	10	30	0.8735
5	10	30	0.0925
10	10	30	0.0024
1	5	75	0.9579
5	5	75	0.3948
10	5	75	0.0605
1	5	30	0.9662
5	5	30	0.4665
10	5	30	0.0925

The dyed, index-matched colloidal crystal of PMMA colloidal particle will also operate as an optical limiter that

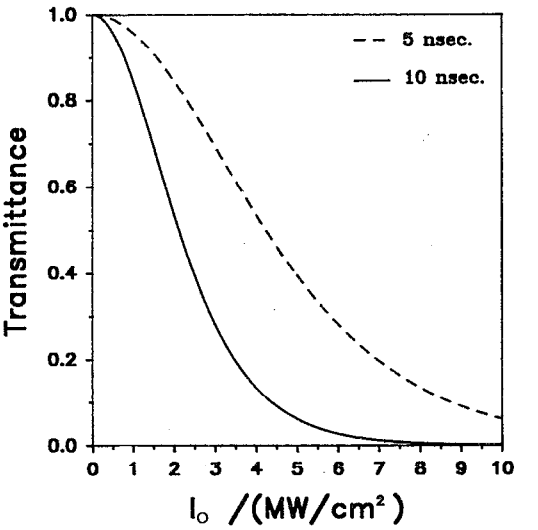

FIG. 7. Transmittance of the probe beam of wavelength 514.5 nm incident at the Bragg angle $\theta_B = 75°$ as a function of the incident beam intensity for the pulse durations t_h of (—) 10 ns and (---) 5 ns, through an index-matched 400-μm-thick colloidal bcc crystal of 83-nm-diam dyed PMMA particles. The transmittance plotted is that occurring at the trailing edge of the pulse.

Downloaded 23 Jan 2009 to 130.49.228.46. Redistribution subject to AIP license or copyright; see http://jap.aip.org/jap/copyright.jsp

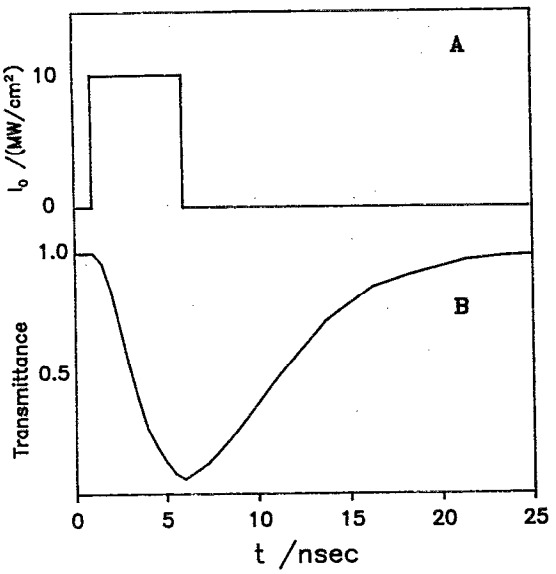

FIG. 8. Time dependence of transmittance through a nonlinear optical switch. (a) Heat beam pulse shape. (b) Transmission of the probe beam of wavelength 514.5 nm incident at $\theta_B = 75°$ on an index-matched dyed colloidal crystal of 83-nm-diam PMMA particles as a function of time.

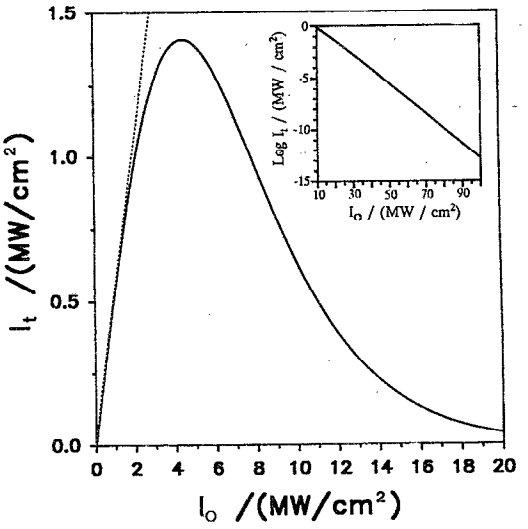

FIG. 10. The dependence of the transmitted intensity as a function of incident intensity for the colloidal crystalline array optical limiter. Incident wavelength $\lambda_h = 450$ nm. The transmitted intensity is calculated at a time 10 ns after the incident beam is turned on. The optical limiter consists of a 50-μm-thick dyed, index-matched PMMA fcc colloidal crystal with particle diameter of 83 nm. $\theta_B = 90°$. The dashed line indicates the transmitted intensity for light that is not diffracted by the lattice. The inset shows the transmitted intensity in log scale as a function of the incident intensity for high intensities.

nonlinearly prevents transmission of high incident intensities. For example, let a heat beam of $\lambda_h = 450$ nm be incident normally on a PMMA colloidal crystal of 50 μm thickness. If each sphere absorbs 1% of the light falling on it, the transmission of the incident heat beam is calculated by Eqs. (35) and (36) to be limited to 0.55 due to light absorption. In addition, if the Bragg condition is satisfied, transmission decreases further due to the Bragg diffraction losses. Assuming that Bragg diffraction, absorption, and scattering act as independent processes, the total transmission of the incident beam is obtained by multiplying the transmittance from incomplete Bragg diffraction by that which results from light absorption (0.55). The ratio of the Bragg diffracted power to the incident power is given by Eqs. (29)–(38), with λ_p in Eqs. (33) and (38) replaced by λ_h. Figure 9 shows the time dependence of the transmission of a 10-MW/cm^2 continuous wave heat beam of $\lambda_h = 450$ nm through the 50-μm-thick dyed, index-matched PMMA crystal which satisfies the Bragg condition for $\theta_B = 90$. The transmittance decreases to 1% within 16 ns, and decreases exponentially to 10^{-10} in 68 ns. Figure 10 shows the incident intensity dependence of the transmitted intensity through this optical limiter at 10 ns after activation. The transmitted intensity decreases to 10 kW/cm^2 for an approximately 25-MW/cm^2 incident beam and decreases to 10 μW/cm^2 for an 80-MW/cm^2 incident beam. At low incident intensities the transmittance remains high. The dashed line indicates the expected linear transmittance in the absence of Bragg diffraction which is attenuated only by sphere absorption. Obviously, this optical device shows unique promise for use as an optical limiter to nonlinearly prevent transmission of intense incident laser radiation.

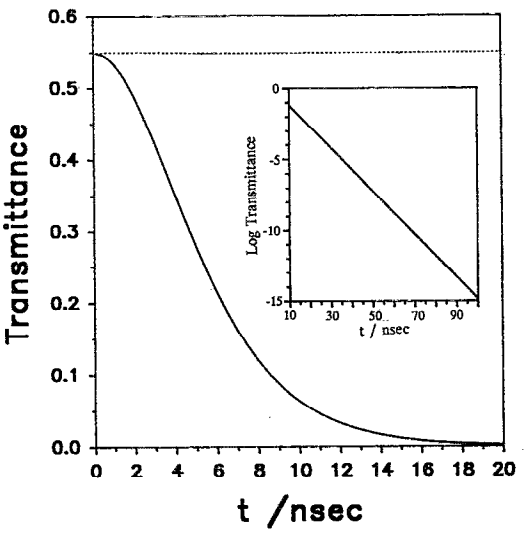

FIG. 9. The transmittance of a nonlinear optical limiter of an incident beam of wavelength $\lambda_h = 450$ nm, of intensity 10 MW/cm^2 through a 50-μm-thick dyed, index-matched PMMA fcc colloidal crystal (with particle diameter of 83 nm) at 90° as a function of time, (—) when Bragg condition is satisfied, and (—) when Bragg condition is not satisfied. Inset shows the log of transmittance as a function of time.

V. CONCLUSION

The three-dimensional heat conduction equation has been solved for a hot sphere cooling in an infinitely extended aqueous medium. The temperature field as a function of time and position in the sphere as well as in the medium is obtained by a Laplace transformation tech-

Downloaded 23 Jan 2009 to 130.49.228.46. Redistribution subject to AIP license or copyright; see http://jap.aip.org/jap/copyright.jsp

nique. The temperature in the medium decreases exponentially with the radial distance from the surface of the sphere. The particle temperature at the surface is lower than that at the center. The PMMA particle of 83 nm heated to 120 °C is found to cool off within 7 ns in water causing the water temperature at the sphere surface to increase to a maximum of $\sim$ 5 °C. This temperature rise decays in 17 ns. The cooling time decreases quadratically with the sphere diameter. We discuss the use of this rapid thermal response as the basis for a novel optical limiter device and for uses in ns optical monostable switching devices and optical monostables.

[1] W. B. Russel, D. A. Saville, and W. R. Schowalter, *Colloidal Dispersions* (Cambridge University Press, New York, 1989).
[2] D. Thirumalai, J. Phys. Chem. **93**, 5637 (1989).
[3] M. O. Robbins, K. Kremer, and G. S. Grest, J. Chem. Phys. **88**, 3286 (1988).
[4] Y. Monovoukas and A. P. Gast, J. Colloid Interface Sci. **128**, 533 (1989).
[5] S. A. Asher, U.S. Patents No. 4,627,689 and No. 4,632,517 (December 1986).
[6] P. L. Flaugh, S. E. O'Donnell, and S. A. Asher, Appl. Spectrosc. **38**, 847 (1984).
[7] R. Kesavamoorthy, M. Rajalakshmi, and C. Babu Rao, J. Phys. Condens. Matter **1**, 7149 (1989).
[8] W. Härtl and H. Versmold, J. Chem. Phys. **80**, 1387 (1984).
[9] P. A. Rundquist, P. Photinos, S. Jagannathan, and S. A. Asher, J. Chem. Phys. **91**, 4932 (1989).
[10] M. Kerker, *The Scattering of Light and Other Electromagnetic Radiation* (Academic, New York, 1969).
[11] W. H. Zachariasen, *Theory of X-ray Diffraction in Crystals* (Wiley, New York, 1945).
[12] P. A. Gohman, G. Bambakidis, and R. J. Spry, J. Appl. Phys. **67**, 40 (1990).
[13] P. A. Rundquist, S. Jagannathn, R. Kesavamoorthy, C. Brnardic, S. Xu, and S. A. Asher, J. Chem. Phys. **94**, 711 (1991).
[14] R. Kesavamoorthy, S. Jagannathan, P. A. Rundquist, and S. A. Asher, J. Chem. Phys. **94**, 5172 (1991).
[15] N. Dovichi, CRC Crit. Rev. Anal. Chem. **17**, 357 (1987).
[16] H. Eichler, G. Salje, and H. Stahl, J. Appl. Phys. **44**, 5383 (1973).
[17] F. B. Hildebrand, *Advanced Calculus for Applications* (Prentice-Hall, New Jersey, 1962).
[18] W. van Megen, S. M. Underwood, and I. Snook, J. Chem. Phys. **85**, 4065 (1986).
[19] W. Wunderlich, in *Polymer Handbook*, edited by J. Brandrup (Wiley International, New York, 1989), p. v/77.
[20] D. Harvey, A. Bader, and J. Nagarkatti, *Aldrich Catalog Handbook of Fine Chemicals* (Aldrich Chemical Company, Wisconsin, 1988).
[21] P. A. Rundquist, R. Kesavamoorthy, S. Jagannathan, and S. A. Asher, J. Chem. Phys. **95**, 1249 (1991).

Downloaded 23 Jan 2009 to 130.49.228.46. Redistribution subject to AIP license or copyright; see http://jap.aip.org/jap/copyright.jsp